

Exploring novel arterio-venous graft designs to reduce vascular access failure risk

G. De Nisco¹, K. Siciliano¹, P. Tasso¹, M. Lodi Rizzini¹, V. Mazzi¹, K. Calò¹,
M. Antonucci², D. Gallo¹, and U. Morbiducci¹

¹ Polito^{BIO}Med Lab, Department of Mechanical and Aerospace Engineering, Politecnico di Torino, Turin, Italy

² Cardiovascular Lab SpA, Milan, Italy

Abstract—Although arterio-venous grafts (AVGs) are the second best option as permanent vascular access for hemodialysis, this solution is still affected by a relevant failure rate associated with neointimal hyperplasia (IH), mainly located at the venous anastomosis, where abnormal hemodynamics occurs. In this study we use computational fluid dynamics (CFD) to investigate the impact of six innovative AVG designs on reducing the IH risk at the distal anastomosis in AVGs. Findings from simulations clearly show that using a helical-shaped flow divider located in the venous side of the graft could assure a reduced hemodynamic risk of failure at the distal anastomosis, with a clinically irrelevant increase in pressure drop over the graft.

Keywords—AVG, hemodialysis, helical flow, neointimal hyperplasia.

I. INTRODUCTION

PATIENT affected by end stage renal disease (ESRD) are in need of a permanent vascular access, assuring an effective hemodialysis treatment [1]. In hemodialysis, when arterio-venous fistula placement is not possible (e.g., in elderly or diabetics) AVG represents the second-best option. Technically, an AVG approach is based on a synthetic graft surgically connecting an artery with a vein, usually in the arm [1]. Unfortunately, the clinical use of the AVG is still affected by a not negligible failure rate, and is markedly associated with thrombus formation in the graft and progressive IH, mainly at the venous anastomosis [1][2].

Abnormal hemodynamics has been proposed as a primary promoter of IH at the distal vein [2], where the luminal surface experiences low and oscillatory wall shear stress (WSS). Evidences of a hemodynamic risk of failure has stimulated the hemodynamic optimization of AVG design. In particular, the documented physiological significance of helical flow in main arteries [3]-[6] has led to rethink AVGs in terms of helical blood flow induction, attempt an improvement of their performance [7][8]. Findings from previous studies reported that: (1) the use of helical-shaped grafts reduces IH risk, with respect to conventional straight grafts [7]; (2) the helical flow intensity at the distal anastomosis of AVG depends on helix turns number or amplitude of helical-shaped graft [8]. However, the beneficial effect of helical-shaped grafts could be affected by an *in vivo* deformation of the helical geometry, a problem still open because of the superficial implantation of these devices.

Here we adopted CFD to characterize the hemodynamic performance of six innovative AVG designs in a closed-loop configuration, aiming at preserving/improving the beneficial impact of helical flow in reducing the IH risk at the distal

anastomosis in AVGs.

II. MATERIALS AND METHODS

Eight different idealized 3D graft models connecting an artery and a vein in a closed-loop configuration were created in Solidworks (Fig.1). Two of them reproduce the design of conventional AVGs (i.e., the straight conventional graft - S-AVG, and the SwirlGraft™ - H-AVG), and used as reference standard. The other six models presented an innovative design. More in detail, the section of the grafts was divided into three equal parts by positioning a flow divider (FD), as shown in Fig.1. For three of the six models, named as linear flow divider (LFD) models, the FD was not rotated along the centerline of the graft, while in the other three models, named as helical flow divider (HFD) models, the FD is rotated while translated along the graft section, describing three helically shaped segments around the graft centerline. Three alternative AV design were considered both for the LFD and HFD solution, as shown in Fig.1.

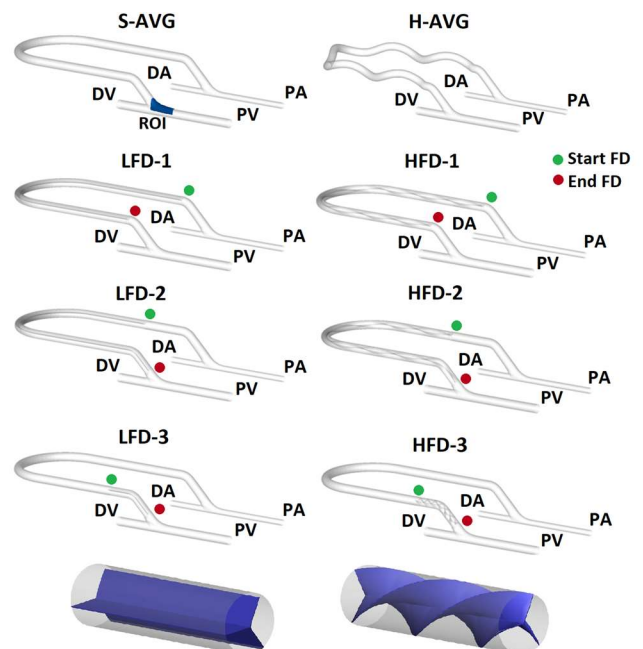


Figure 1. Investigated AV graft models. Green and red markers indicate the proximal and the distal end of the graft segment equipped with the FD, respectively. The two types of FD positioning are also shown (bottom panel).

The Navier-Stokes equations were numerically solved using the finite volume-based CFD code Fluent on discretized AVG fluid domains, with tetrahedral elements in the lumen region, and high-quality prismatic elements in the near wall region. The same scheme already proposed elsewhere was applied to define conditions at boundaries [8].

Hemodynamic Descriptors

WSS-based descriptors of ‘disturbed flow’ was used to analyse near-wall hemodynamics (Table I): time-averaged wall shear stress (TAWSS), oscillatory shear index (OSI), and relative residence time (RRT). The analysis was focused at the region of interest (ROI) at the venous anastomosis. Data from all cases were combined to define objective thresholds for ‘disturbed flow’: the upper (lower) 20th percentile was identified for OSI and RRT (TAWSS) [5]. For each model, the percentage of ROI surface area (SA) exposed to OSI and RRT values higher (lower for TAWSS) than the defined thresholds was quantified and respectively labeled as OSI80, RRT80, and TAWSS20. To compare all eight cases, the percentage difference in the mean value of each WSS-based descriptor at the ROI with respect to the conventional models was quantified. Intravascular hemodynamics was investigated in terms of cycle-average helicity intensity (h_2 in Table I) [3], recognized to reduce the hemodynamic risk of failure in AVGs [7][8]. Additionally, the potential thrombus formation risk in the graft was quantified in terms of volume of recirculating flow (VolRec) [4], in order to analyse the risk of blood clotting in the graft commonly associated with commercial devices.

TABLE I

NEAR-WALL AND INTRAVASCULAR HEMODYNAMIC DESCRIPTORS

TAWSS	$\text{TAWSS} = \frac{1}{T} \int_0^T \mathbf{WSS} dt$
OSI	$\text{OSI} = 0.5 \left[1 - \frac{\left \int_0^T \mathbf{WSS} dt \right }{\int_0^T \mathbf{WSS} dt} \right]$
RRT	$\text{RRT} = \frac{1}{\frac{1}{T} \int_0^T \mathbf{WSS} dt}$
h_2	$h_2 = \frac{1}{TV} \int_T \int_V \mathbf{v} \cdot \boldsymbol{\omega} dV dt$

\mathbf{WSS} is the WSS vector; T is the period of the cardiac cycle; V is the model volume; \mathbf{v} is the velocity vector; $\boldsymbol{\omega}$ is the vorticity vector.

III. RESULTS

A direct comparison of designed grafts with S-AVG and H-AVG is provided by Fig. 2, reporting the percentage differences in WSS-based descriptors values averaged over the ROI surface area. It emerges that (1) H-AVG presents better performances than S-AVG; (2) LFD models have poorer performance than commercially available models; (3) models HFD-1 and HFD-2 perform overall less effectively than S-AVG and H-AVG; (4) case HFD-3 ROI-average TAWSS values are 38.8% and 34.2% higher than S-AVG and H-AVG models, respectively. This suggests higher performance for case HFD-3 than S-AVG and H-AVG, in terms of IH hemodynamic risk at the venous anastomosis.

To complete the hemodynamic characterization of the different AVG designs, the risk of thrombus formation in terms of VolRec amount, and the cycle-average pressure drops over the graft segment were computed. It can be noted that the percentage volume of recirculation in the graft is low in all the investigated model and not markedly affected by FD insertion (Table II). As for pressure drops, the insertion of the FD and the helically-shaped geometry slightly affects the

energetics of blood flowing in the graft. In particular, case HFD-3 exhibits an increase in pressure drop of 3.8 mmHg and 2.0 mmHg than S-AVG and H-AVG, respectively.

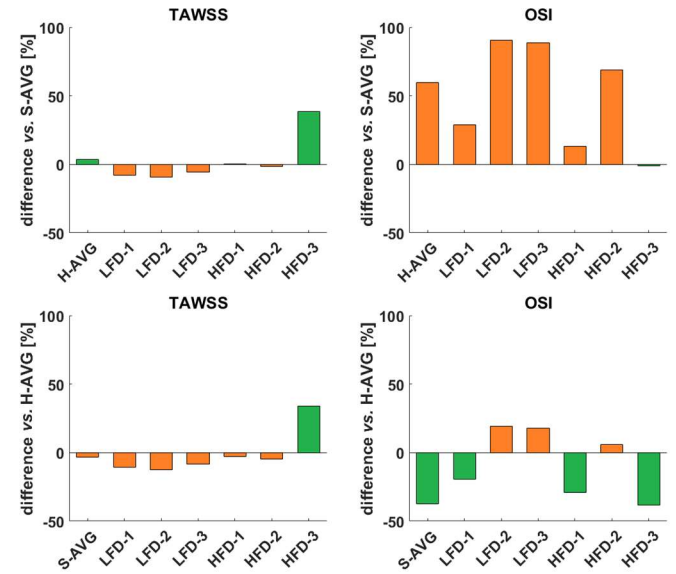


Figure 2. Percentage difference in mean values of WSS-based descriptors at ROI compared to: top) S-AVG model; bottom) H-AVG model. Beneficial effects are green-coloured; detrimental effects are orange-coloured.

TABLE II

NORMALIZED VOLUME OF RECIRCULATING FLOW AT THE GRAFT SEGMENT

S-AVG	H-AVG	LFD-1	LFD-2	LFD-3	HFD-1	HFD-2	HFD-3
0.41%	0.82%	0.29%	0.32%	0.37%	0.28%	0.31%	0.52%

IV. CONCLUSION

These findings confirm that designing AVG as helical blood flow inducer could reduce the hemodynamic-based IH risk at the venous anastomosis of AVGs, without markedly increasing pressure drop and the risk of thrombus formation.

REFERENCES

- [1] B. Ene-Iordache, and A. Remuzzi, “Blood flow in idealized vascular access for hemodialysis: a review of computational studies”, *Card. Eng. Tech.*, vol. 8(3), pp. 295-312, 2017.
- [2] F. Loth, P.F. Fischer, N. Arslan, C.D. Bertram, S.E. Lee, T.J. Royston, W.E. Shaalan, and H.S. Bassiouny, “Transitional flow at the venous anastomosis of an arteriovenous graft: potential activation of the ERK1/2 mechanotransduction pathway”, *J. Biomech. Eng.*, vol. 125(1), pp. 49-61, 2003.
- [3] D. Gallo, D.A. Steinman, P.B. Bijari, and U. Morbiducci, “Helical flow in carotid bifurcation as surrogate marker of exposure to disturbed shear”, *J. Biomech.*, vol. 45, pp. 2398-2404, 2012.
- [4] D. Gallo, P.B. Bijari, U. Morbiducci, Y. Qiao, Y. Xie, M. Etesami, D. Haabets, E.G. Lakatta, B.A. Wasserman, and D.A. Steinman, “Segment-specific associations between local haemodynamic and imaging markers of early atherosclerosis at the carotid artery: an in vivo human study”, *J. R. Soc. Interface*, vol. 15(147), 2018.
- [5] U. Morbiducci, R. Ponzini, M. Grigioni, and A. Redaelli, “Helical flow as fluid dynamic signature for atherogenesis in aortocoronary bypass. A numeric study”, *J. Biomech.*, vol. 40, pp. 519-534, 2007.
- [6] G. De Nisco, A.M. Kok, C. Chiastra, D. Gallo, A. Hoogendoorn, F. Migliavacca, J.J. Wentzel, and U. Morbiducci, “The atheroprotective nature of helical flow in coronary arteries”, *Ann. Biomed. Eng.*, vol. 47(2), pp. 425-438, 2019.
- [7] C. Caro, N. Cheshire, and N. Watkins, “Preliminary comparative study of small amplitude helical and conventional ePTFE arteriovenous shunts in pigs”, *J. R. Soc. Interface*, vol. 2, pp. 261-266, 2005.
- [8] K. Van Canneyt, U. Morbiducci, S. Eloot, G. De Santis, P. Segers, and P. Verdonck, “A computational exploration of helical arterio-venous graft designs”, *J. Biomech.*, vol. 46(2), pp. 345-353, 2013.